Journal of Computer Engineering
ISSN 10003428

Original Research Article
Vol 9, Issue 1, 2020 | ISSN: 1000-3428

Investigation of Anomalous Transport Phenomena in Power Law Fluids under Combined Electroosmotic and Pressure-Driven Flow Conditions

Dr. Rohan K. Desai, Dr. Kavita R. Mehta, Dr. Avijit Sengupta

Department of Chemical Engineering, Indian Institute of Technology Kharagpur, West Bengal, India; Department of Mechanical Engineering, Indian Institute of Technology Bombay, Maharashtra, India

Abstract—In this study, we have analyzed the transport of analytes under a two dimensional steady incompressible flow of power-law fluids through rectangular nanochannel. A mathematical model based on the Cauchy momentum-Nernst-Planck-Poisson equations is considered to study the combined effect of mixed electroosmotic (EO) and pressure driven (PD) flow. The coupled governing equations are solved numerically by finite volume method. We have studied extensively the effect of key parameters, e.g., flow behavior index, concentration of the electrolyte, surface potential, imposed pressure gradient and imposed electric field strength on the net average flow across the channel. In addition to study the effect of mixed EOF and PD on the analyte distribution across the channel, we consider a nonlinear model based on general convective-diffusion-electromigration equation. We have also presented the retention factor for various values of electrolyte concentration and flow behavior index.

I. Introduction

HEN the electrolyte in a channel comes in contact with a solid wall, a static charge develops along the solid surface. The charged surface attracts counterions and an electric double layer (EDL) forms along the surface. An EDL consisting of a stern layer and a diffuse layer in which the ions are loosely connected under the action of an externally imposed electric field tangential to the surface, the surplus counterions in the diffused double layer experiences a Columbic force and starts moving towards the electrode of opposite sign, which in turn results in an electroosmotic flow [1]- [3]. From last decade, the study on Electroosmotic flow (EOF) paid great attention due to its numerous applications in the field of biological analysis and chemical process. In addition the floe behaviour can also be applied in microfluidic and nanofluidic devices as a pumping method with the fast development of the lab-on-a-chip technology [4], [5].

There have been a number of investigations on EOF due to non-Newtonian fluids with various type of non-Newtonian constitutive models such as power-law model [6], Carreau model [7], Bingham model [8] and Moldflow first-order model [9] etc. The power-law model is most preferred because of its simplicity and its ability to characterize a wide range of non-Newtonian fluids [10]. This model canproperly describe the effects of apparent viscosity of a sample non-Newtonian fluid on the flow behavior. Several authors studied the EOF based on the Poisson-Boltzmann model in which the distribution of ions is assumed to governed by the equilibrium Boltzmann distribution. Das and Chakraborty [11] obtained an analytical solution to describe the electrokinetic transport of a non-Newtonian fluid flow in a microchannel. Zhao et al. [12] analyzed the EOF of power-law fluids in a silt microchannel and derived analytical solutions for the share stress, effective viscosity and velocity profile distribution through the Debye-H*u*¨ckel approximation under a low surface potential assumption [13]. Tang et al. [14] analyzed numerically the EOF of non-Newtonian fluids by using the Lattice-Boltzmann method and found that a significant effect of the fluid rheological behavior on the flow pattern. Vasu and De [15] presented a mathematical model for pure EOF of power-law fluids in a rectangular microchannel at high zeta potential without invoking the Debye-H*u*¨ckel approximation.

Recently several authors studied the mixed EOF and pressure driven (PD) flow. One important aspect of mixed EOF and PD flow is to regulate the flow behaviour by imposing the external pressure gradient. Babaie et al. [16] solved numerically the combined EOF and PD flow of power-law fluids in a silt microchannel. The separation of analytes ions in nanochannels systems with mixed EOF and PD flow studied by Pennathur and Santiago [17], Griffiths and Nilson [18] and Xuan et al. [19]. They determined the general trends and conditions to achieve maximum separation in nanofluidic channels using this combined EOF and PD flow approach.

In the present study, we have analyzed the transport of analytes under mixed EOF and PD flow of power law fluid. We have studied extensively the effect of key parameters, e.g., flow behavior index, concentration of the electrolyte, surface potential, imposed pressure gradient and imposed electric field strength on the net average flow across the channel. We also studied the variation of retention factor with concentration of electrolyte for various values of flow behavior index. The characteristics of the electrokinetic flow are obtained by numerically solving the Nernst-Planck equation, Poisson equation and the general Cauchy

How to cite: Dr. Rohan K. Desai, Dr. Kavita R. Mehta, Dr. Avijit Sengupta (2020). Investigation of Anomalous Transport Phenomena in Power Law Fluids under Combined Electroosmotic and Pressure-Driven Flow Conditions. Journal of Computer Engineering, 9(1), 53–61. DOI: https://doi.org/10.5281/zenodo.19341319

momentum equation, instead of the Navier-Stokes equation, simultaneously.

II. Mathematical Model

In this study we consider the transport of analytes under a two dimensional steady incompressible flow of Power law fluid through rectangular nanochannel (Fig. 1). The channel walls are considered to bear a constant surface potential ζ. The electric field of strength E_0 applied externally along the axis of the channel. To neglect the channel edge effect we consider the channel width (w) is much higher than the channel height (H). The fluid flow considered to be generated due to the externally applied electric field and applied pressure gradient. Below we summarize the governing equations for mixed electrosmotic and pressure driven (PD) flow.

Fig. 1 Schematic representation of the nanochannel used for the analysis

The nondimensioanal form of the governing equation for electric potential can be written as

(1)

Here the electric potential φ is scaled by $\varphi_0 = RT/F$, where R, T and F are gas constant, absolute temperature and Faraday constant, respectively. The spatial coordinates are scaled by H. We have chosen binary symmetric electrolyte with valence $z_i(i = 1,2) = \pm 1$. The ion concentrations are scaled by the bulk number concentration of ions n_0. Here $n_i(i = 1,2)$ are the number concentration and z_i is the valence of the i^{th} ionic species. The Debye length thickness κ^{-1} is defined as

, where k_B is the Boltzmann constant, e is the elementary electric charge and ε_e is the permittivity of the medium.

The concentration of ionic species are governed by the general convective-diffusive-electromigration process i.e., by Nernst-Plank equation. The nondimensional form of transport equation of i^{th} ionic species can be written as

Here time is scaled by H/u_s and u = (u,v) is the velocity [1]

vector scaled by u_s, where is the generalized Helmholtz-Smoluchowski (HS) velocity for power law fluid, where m is the flow consistency index and n is the flow behavior index. Depending on the values of n, the shear thinning ($n < 1$), shear thickening ($n > 1$) and Newtonian ($n = 1$) behavior can be observed. We denote u_0 as the corresponding HS velocity for Newtonian fluid (n=1). The Peclet number is defined as Pe = Re.Sc with $Re = \rho u_s^{2-n} H^n/m$ is the Reynolds number and Schimdt number $Sc = m(\frac{u_s}{H})^{n-1}/\rho D_i$ where D_i is the diffusivity of the i^{th} type species, ρ is the density of the fluid and $\Lambda = E_0 H/\varphi_0$ is the scaled applied strength.

The non-dimensional form of fluid flow equation for power law fluid can be written as

$$\frac{\partial u}{\partial x} + \frac{\partial v}{\partial y} = 0 \tag{3}$$

$$Re(\frac{\partial u}{\partial t} + u\frac{\partial u}{\partial x} + v\frac{\partial u}{\partial y}) = -\frac{\partial p}{\partial x} + \eta(\frac{\partial^2 u}{\partial x^2} + \frac{\partial^2 u}{\partial y^2}) + 2\frac{\partial \eta}{\partial x}\frac{\partial u}{\partial x}$$

$$+\frac{\partial \eta}{\partial y}(\frac{\partial u}{\partial y} + \frac{\partial v}{\partial x}) + \frac{(\kappa H)^{n+1}}{2\Lambda\zeta n^n}(n_1 - n_2)(\frac{\partial \phi}{\partial x} - \Lambda) \tag{4}$$

$$Re(\frac{\partial v}{\partial t} + u\frac{\partial v}{\partial x} + v\frac{\partial v}{\partial y}) = -\frac{\partial p}{\partial y} + \eta(\frac{\partial^2 v}{\partial x^2} + \frac{\partial^2 v}{\partial y^2}) + 2\frac{\partial \eta}{\partial y}\frac{\partial v}{\partial y}$$

$$+\frac{\partial \eta}{\partial x}(\frac{\partial u}{\partial y} + \frac{\partial v}{\partial x}) + \frac{(\kappa H)^{n+1}}{2\Lambda\zeta n^n}(n_1 - n_2)\frac{\partial \phi}{\partial y} \tag{5}$$

We consider $m(\frac{u_s}{H})^n$ as the pressure scale. The non-dimensional form of dynamic viscosity (η) of the power-law fluid can be written as

$$\eta = \left[2(\frac{\partial u}{\partial x})^2 + 2(\frac{\partial v}{\partial y})^2 + (\frac{\partial u}{\partial y} + \frac{\partial v}{\partial x})^2\right]^{\frac{(n-1)}{2}} \tag{6}$$

where η is scaled by $m\left(\frac{u_s}{H}\right)^{n-1}$.

We impose no slip boundary condition along the channel walls. The channel walls are kept as a constant surface potential ζ and walls are considered to be ion impenetrable, i.e., the molar flux of the ionic species is considered to be zero along the channel walls. We consider a fully developed boundary conditions along the inlet and outlet of the channel. For mixed EOF and PD flow, we consider an external pressure gradient G imposed along x- direction where the nondimensional pressure gradient, scaled by mu^n_s/H^{n+1}, is given by

$$G = -\left(\frac{n}{n+1}\right)^n \frac{H^{n+1}}{mU_s^n}\frac{dp}{dx} \tag{7}$$

A. Analyte Distribution

The analytes we are investing are at trace concentration compared to the buffer electrolyte. The governing equation

for analyte distribution can be written in nondimensional form as

$$Pe\frac{\partial n_s}{\partial t} - \nabla^2 n_s - z_s \nabla . n_s \nabla \phi + Pe\nabla .(n_s \mathbf{u}\ ) = 0 \quad (8)$$

where n_s and z_s are the ionic concentration and valence of the analyte, respectively. We consider bulk value of the analyte concentration $n^o{}_s$ as we scale for ionic concentration of the analyte. To neglect the effect of analyte concentration on the overall electrolyte concentration, we consider the analyte concentration much lower than the buffer electrolyte. The governing equation of analyte concentration is solved with the known potential and velocity distribution across the channel. We impose a symmetry boundary condition along the inlet and outlet of the channel. The molar flux of the analyte species is taken to zero along the channel wall.

III. Numerical Methods

The governing equations for ionic concentration, induced potential and fluid flow are solved numerically using a control volume approach [20] over a staggered grid where the velocity components are stored at the midpoints of the cell sides to which they are normal. The scalar quantities such as the pressure and concentrations are stored at the center of the cell. The discretized form of the governing equations is obtained by integrating the governing equations over each control volume.

The fluid flow equations are coupled with equations for ionic concentration, induced potential equation through the electric body force term. On the other hand, Poisson equation for potential field is coupled with the Nernst-Planck equation via the net charge density as its source term. In addition Nernst-Planck equations are also coupled with both the potential and velocity field. Hence, to solve the governing equations in a coupled manner, we need to develop an iterative scheme. The successive steps for solving the governing equations can be summarized as:

1) Solve the Poisson equation for induced potential.
2) With known potential and guessed velocity field, solve the Nernst-Planck equations for for ionic concentration.
3) With known potential and concentration field solve the the equation fluid flow equations using SIMPLE algorithm (Patankar, [21]).
4) Repeat steps 1-3 until it meets the tolerance limit (10^{-6}) to get required velocity, potential and concentration field.
5) Repeat steps 1-4 until we achieve a steady state velocity, potential and concentration field.

With the known velocity and potential field we have solved the governing equation for analyte distribution. In order to validate our numerical scheme, a comparison of the streamwise velocity component for fully developed EOF for power law fluid is made with analytical result due to Zhao et al. [12]. It may be noted that the results of Zhao et al. [12] are based on Poisson- Boltzman (PB) model under low potential limit where the ionic concentrations of are followed from Boltzman distribution. We found our computed results (Fig. 2) based on Poisson-Nernst-Planck (PNP) model are in good agreement with the results due to Zhao et al. [12] for strong electrolyte solution. In addition we have also shown a comparison (Fig. 4) for the retention factor for the analyte distribution with the existing solution due to Griffiths and Nilson [18] for Newtonian case (n = 1). A detailed discussion on retention can be found later to this article.

IV. Results and Discussion

In the present study, we consider the height of the channel as 50 nm. The flow consistency index is taken to be m=0.001 pa.s^n with fluid density ρ = 1000 kg/m^3. The mass diffusion coefficient for both the ions are assumed to be same as $D_+ = D_- = D = 2 \times 10^{-9}$ m^2/s. We consider surface potential along the channel walls as -0.025 v and the range for the applied electric field strength E_o is varied from cases to case in between 10^4 to 10^6 v/m. The Debye Huckel parameter κh is varried from 1 to 50 by varrying the solution concentration for fixed channel height (H= 50 nm). The flow behavior index (n) is considered to be ranges from 0.8 to 1.5.

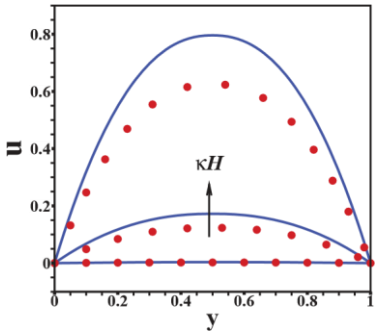

(a) $n = 0.8$

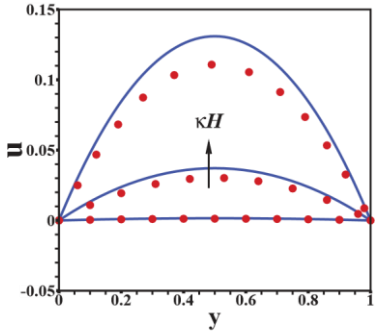

(b) $n = 1.0$

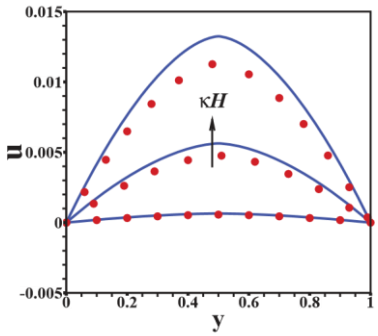

(c) $n = 1.5$

Fig. 2 Comparison of the present axial velocity (lines) with the analytic results (symbols) presented by Zhao et al. [12] for various values of flow behavior index (a) n=0.8, (b) n=1.0 and (c) n= 1.5 with fixed values of κH=0.1, 0.5, 1, ζ=-1, $E_o = 10^4$ v/m and channel height H = 50 nm

To start with we first consider the pure EOF (in absence of external pressure gradient). We present the stremwise velocity $u(y)$ for three different values of Debye Huckel parameter (κH=0.1, 0.5 and 1) in Figs. 2(a)-(c). For the sake of simplicity, we consider the Newtonian HS velocity u_o, as the velocity scale for all results. Here we consider three different types of fluids, i.e., n = 0.8(< 1, for pseudoplastic fluids); n = 1 (for Newtonian fluid) and n = 1.5(> 1, for dilatant fluids). In each case we found a nearly parabolic shape of the axial velocity profile for purely EOF case at lower values of the electrolyte concentration. We have also presented corresponding analytical solution based on Poison Boltzmann (PB) model due to Zhao et al. [12] under a low potential limit.

We see that our results overpredict with the analytic results for lower values of electrolyte concentration. From Figs. 2(a)-(c), we see that a discrepancy between the PNP model and PB model occurs at low electrolyte concentration (lower values of κH) and it occurs due to the overlapping of the adjacent EDLs.

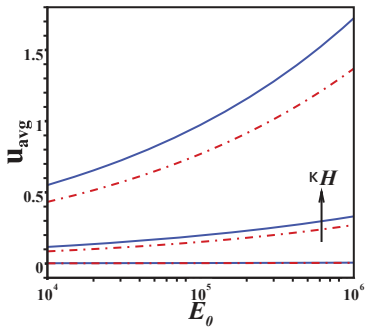

(a) n = 0.8

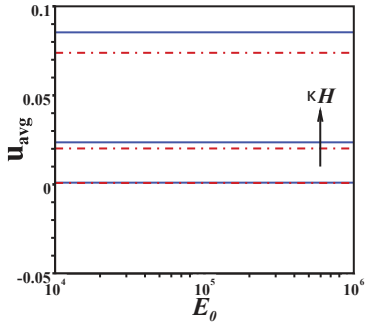

(b) n = 1.0

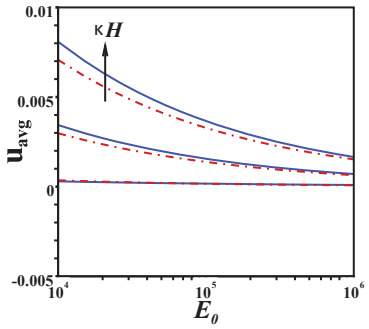

(c) n = 1.5

Fig. 3 Variation of average velocity (u_{avg}) with external electric field (E_o) for different values of flow behavior index with fixed κH =0.1, 0.5 and 1, $E_o = 10^4$ v/m, G = 0 and channel height H = 50nm. Here dashed lines present the analytic results presented by Zhao et al. [12]

Fig. 3 presents the variation of average velocity with the external electric field for different values of κH = with three values of flow behavior index (n). The average velocity (u_{avg}) increases monotonically for increasing electrolyte concentration. For flow behavior index $n \leq 1$, the increase in κH leads to an increment in electric driving force and decrease in wall viscosity and results an increment in average velocity. On the otherhand n >1, the wall viscosity is enough to overcome the increasing body force with the

increase in electrolyte concentration and it leads to a relative smaller value of u_{avg}. We also found an increment in the value of u_{avg} with E_0 for n <1. On the otherhand for n >1, the value of u_{avg} decreases with the increase in E_0.

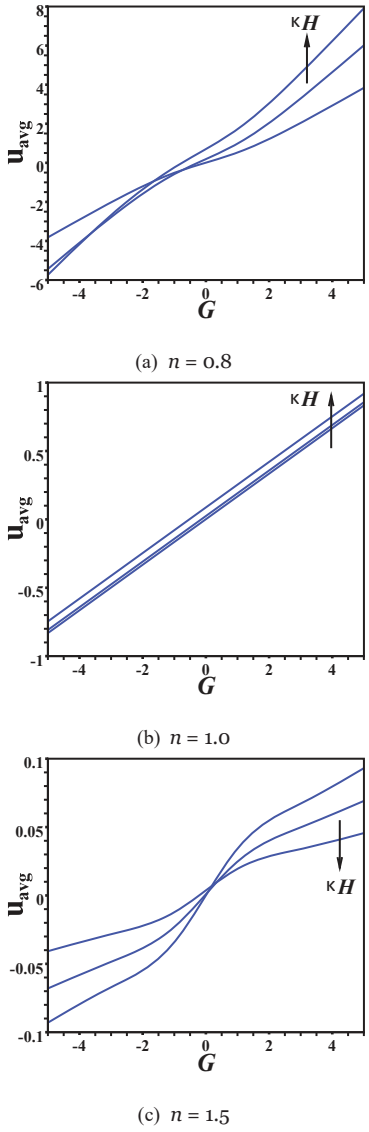

(a) n = 0.8

(b) n = 1.0

(c) n = 1.5

Fig. 4 Variation of average velocity (u_{avg}) with pressure gradient (G) for different values of flow behavior index with fixed ζ = −=150, κHnm =0.1, 0.5 and 1, E_0 = 10$_4$ v/m and channel height H

Here we consider the mixed pressure driven (PD) and EOF. We represent the variation of u_{avg} with imposed pressure gradient G in Fig. 4 for different values of flow behavior index n. We see that u_{avg} increases with the increase of imposed pressure gradient G. From Fig. 4 we found a decrease in the axial velocity with the increase of flow behavior index n at a given G. The decrease in magnitude of the axial velocity can be justified through the effective viscosity. For increasing values of n, the value of the effective viscosity increases and it leads to a decrement in magnitude of the axial velocity. An interesting feature can be observed from Fig. 4 that the axial velocity increases with the increases in κH for $n \leq 1$ while its decreases with an increment in κH for n >1. It may be noted that for increasing values of κH, the value of the electric body force increases for all the values of flow behavior index parameter n. On the otherhand, the value of wall viscosity is a decreasing function of κH for flow behavior index n <1, while its value increases with the increase in κH for n > 1. Due to combined effect of decreasing wall viscosity and increasing electric driving force with increasing κH, the axial velocity increases for n <1. On contrary the axial velocity becomes an decreasing function of κH for n > 1 as the wall viscosity increases significantly with the increase in κH and it dominates over the electric driving force, and hence leads to a reduction in average flow rate.

In this section, we have studied extensively the combined effect of mixed EOF and PD flow on the analyte distribution. We consider the trace analyte as monovalent charged species with valence z_s = +1 or −1. To study the effect of externally applied electric field and imposed pressure gradient, we varied the values of E_0 and G from case to case. To present a quantitative study on effect of fluid velocity on the electrophoretic migration of analyte though nanochannel, we need to consider the retention factor R_s as the ratio of analytes velocity to the fluid velocity (Pennathur, [22]).

$$R_s = \frac{<< u_s^{total}(y) >>}{< u(y) >} \tag{9}$$

Here $u_s^{total} = u_{ep} + u(y)$, $u(y)$ is the axial velocity under mixed EOF and PD flow, $u_{ep} = z_s \omega_s E_0$ is the electrophoretic velocity of the analyte, $\omega_s = D_s F/RT$ is the electrophoretic mobility with D_s is the diffusivity of the analyte.

Here $< \chi >$ represent the averaged value of the physical quantity and is defined as

$$< \chi >= \frac{1}{2}\int_{-1}^{1} \chi dy \tag{10}$$

In order to present a systematic study of analyte distribution under mixed EOF and PD flow, we compare our results with the exiting model (Griffiths and Nilson [18]), where we set D_s = 0. From the Fig. 5, it is clear that our computed solution agrees well with the existing studies by Griffiths and Nilson [18] for Newtonian case.

To understand the effect of the combined EOF and PD flow on the analyte migration, previous authors [22], [18] considered the retention factor R_s as the measure of the mass transfer rate under the mixed EOF and PD flow. It

may be noted that R_s involves the ratio of analyte velocity as well as average flow rate. In the present scenario for Power law fluid, the average flow rate strongly depends on the flow behavior index n, and it may takes a smaller values for higher values of n, which leads to significantly large values of R_s. From Fig. 5 we see that our results agrees well with the analytic results presented by Griffiths and Nilson [18].

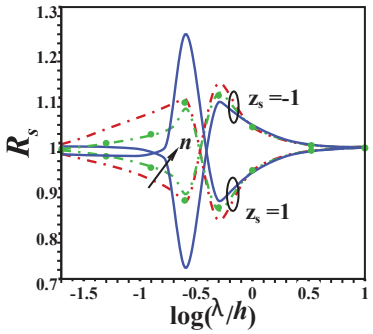

(a) $G = -1$

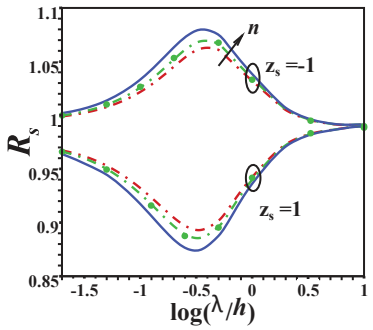

(b) $G = 0$

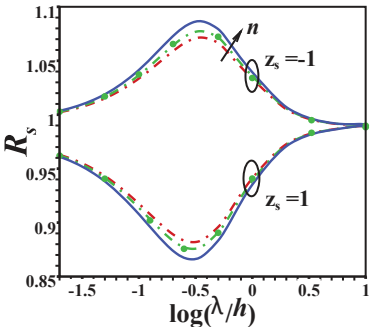

(c) $G = 1$

Fig. 5 Retention versus $\frac{\lambda}{H}$ profile of mixed EOF and PD ($G = -1,0,1$) flow for different values of flow behavior index ($n = 0.8,1.0$ and 1.5) when $D = 0$, $\zeta = -1.0$ and $E_0 = 10_4$ v/m. Here line and symbol present the present model and Griffiths and Nilson [18], respectively

V. Conclusion

In this article, we have studied extensively several aspects of transport of analytes under the influence of mixed elctroosmotic and pressure driven flow. To model the problem we consider the most general convective-electromigration-diffusion equation for concentration distribution, modified Navier-Stokes equation for fluid flow and Poisson equation for double layer potential equation. We employed a numerical scheme based on finite volume method for solving the governing equation though a coupled manner. We found a significant difference in the computed solution from the analytical solution based on several assumptions. In addition we have also considered the transport of analytes under the influence of combined elctroosmotic and pressure driven flow. The results presented in this article suggested that the nonlinear effect due to the fluid convection has significant effect on the flow profile and hence the analyte distribution across the channel.

References

[1] R. J. Hunter, Foundations of colloid science, Oxford University Press, 2001.
[2] R. F. Probstein, Physicochemical hydrodynamics, Wiley, 1994.
[3] J. H. Masliyah, S. Bhattacharjee, Electrokinetic and colloid transport phenomena, John Wiley & Sons, 2006.
[4] H. A. Stone, A. D. Stroock, A. Ajdari, Engineering flows in small devices: microfluidics toward a lab-on-a-chip, Annu. Rev. Fluid Mech. 36 (2004) 381–411.
[5] X. Wang, C. Cheng, S. Wang, S. Liu, Electroosmotic pumps and their applications in microfluidic systems, Microfluidics and Nanofluidics 6 (2) (2009) 145–162.
[6] F. Kamis¸li, Flow analysis of a power-law fluid confined in an extrusion die, International journal of engineering science 41 (10) (2003) 1059–1083.
[7] W. Zimmerman, J. Rees, T. Craven, Rheometry of non-newtonian electrokinetic flow in a microchannel t-junction, Microfluidics and Nanofluidics 2 (6) (2006) 481–492.
[8] M. Das, V. Jain, P. Ghoshdastidar, Fluid flow analysis of magnetorheological abrasive flow finishing (mraff) process, International Journal of Machine Tools and Manufacture 48 (3) (2008) 415–426.
[9] Y. Koh, N. Ong, X. Chen, Y. Lam, J. Chai, Effect of temperature and inlet velocity on the flow of a nonnewtonian fluid, International communications in heat and mass transfer 31 (7) (2004) 1005–1013.
[10] A. Y. Malkin, Rheology Fundamentals, ChemTec, 1994.
[11] S. Das, S. Chakraborty, Analytical solutions for velocity, temperature and concentration distribution in electroosmotic microchannel flows of a non-Newtonian bio-fluid, Analytica Chimica Acta 559 (1) (2006) 15–24.
[12] C. Zhao, E. Zholkovskij, J. H. Masliyah, C. Yang, Analysis of electroosmotic flow of power-law fluids in a slit microchannel, Journal of colloid and interface science 326 (2) (2008) 503–510.
[13] C. Rice, R. Whitehead, Electrokinetic flow in a narrow cylindrical capillary, The Journal of Physical Chemistry 69 (11) (1965) 4017–4024.
[14] G. Tang, X. Li, Y. He, W. Tao, Electroosmotic flow of non-Newtonian fluid in microchannels, Journal of Non-Newtonian Fluid Mechanics 157 (1) (2009) 133–137.
[15] N. Vasu, S. De, Electroosmotic flow of power-law fluids at high zeta potentials, Colloids and Surfaces A: Physicochemical and Engineering Aspects 368 (1) (2010) 44–52.
[16] A. Babaie, A. Sadeghi, M. H. Saidi, Combined electroosmotically and pressure driven flow of power-law fluids in a slit microchannel, Journal of Non-Newtonian Fluid Mechanics 166 (14) (2011) 792–798.
[17] S. Pennathur, J. G. Santiago, Electrokinetic transport in nanochannels. 1. theory, Analytical chemistry 77 (21) (2005) 6772–6781.

[18] S. K. Griffiths, R. H. Nilson, Electroosmotic fluid motion and late-time solute transport for large zeta potentials, Analytical chemistry 72 (20) (2000) 4767–4777.
[19] X. Xuan, D. Li, Solute separation in nanofluidic channels: Pressure-driven or electric field-driven?, Electrophoresis 28 (4) (2007) 627–634.
[20] C. A. Fletcher, Computational techniques for fluid dynamics vol 2, 2nd edn, Springer, Berlin, 1991.
[21] S. Patankar, Numerical heat transfer and fluid flow, CRC Press, 1980.
[22] D. Gillespie, S. Pennathur, Separation of ions in nanofluidic channels with combined pressure-driven and electro-osmotic flow, Analytical chemistry 85 (5) (2013) 2991–2998.